Original Research Article

Omniscient Pte.Ltd.

Verification of seismic enforced-displacement procedure on torsionally flexible, asymmetric, multi-storey r/c buildings

ATHANASIOS P. BAKALIS[1,2], TRIANTAFYLLOS K. MAKARIOS[1,2*]

[1] School of Civil Engineering, Aristotle University of Thessaloniki, Thessaloniki, Greece
[2] Institute of Structural Analysis and Dynamics of Structures, Thessaloniki, Greece

*Correspondence: Triantafyllos K. Makarios, School of Civil Engineering, Aristotle University of Thessaloniki, Thessaloniki, Greece; Email: makariostr@civil.auth.gr

Abstract: A recently proposed direct Displacement-based procedure of nonlinear static (pushover) analysis on multi-storey reinforced concrete (r/c) buildings is verified here against the results of Nonlinear Response History Analysis. An asymmetric, regular in elevation, torsionally flexible, multi-storey r/c building designed according to Eurocode EN 1998 is investigated. Taking fully into account the inelastic torsion and the higher mode effects, as well as the P-Delta effects, the proposed procedure applies a pattern of seismic floor enforced-displacements along the "Capable Near Collapse Principal Axes of the building", aiming at the Near Collapse state. The envelope of the results of sixteen final non-linear static analyses on the investigated building shows that the main aspects of the spatial seismic action effects can be safely captured by the proposed procedure, especially regarding the inelastic interstorey drift ratios, as well as the plastic mechanism of the building.

Keywords: Seismic Enforced-Displacements, Interstorey Drift Ratios, Nonlinear Static Analysis, Pushover Analysis, Response History Analysis, Capable Near Collapse Centre of Stiffness, Torsionally Flexible Building

1. Introduction

The main weakness of the nonlinear static (pushover) procedure proposed by the contemporary seismic codes, as is Eurocode EN 1998-1, is its inability to properly predict the seismic interstorey drift ratios over the height of multistorey r/c buildings. Indeed, the interstorey drift ratios of asymmetric multi-storey buildings are the most representative response measure that controls the distribution of the local inelastic deformations of the structural elements, in plan and in height of the multistorey building, and hence of the structural damage [1-2]. Interstorey drift ratios are usually underestimated by the code-proposed pushover

procedure due to the consideration that the building response is controlled only by the fundamental mode, ignoring the contribution of the higher and torsional modes that develop in the linear area and significantly affect the behavior in the non-linear area of response. Another weakness of the code-proposed pushover procedure is the use of the superposition technique on nonlinear analyses results, into the nonlinear area of response, to consider the spatial seismic action [3]. Additionally, the lack of proposals by the seismic codes about the main loading directions of buildings as well as for the proper consideration of the torsional sensitivity of buildings in pushover analysis raises questions about the correct/rational application of the pushover procedure. The last two issues are directly affected by the lack of definition on the one hand of the real inelastic centre of stiffness and on the other hand of the real inelastic torsional radii of the multi-storey buildings, which are continuously alter in the non-linear response region. These issues have been investigated recently by Bakalis and Makarios [4-8], Makarios and Bakalis [9-11] and Bakalis *et al* [12]. Lastly, P-Delta effects should always be considered in the framework of non-linear analysis, an issue which is not emphasized enough in the seismic codes.

To deal with the inelastic torsion or/and the contribution of higher modes in the linear (and maybe into the nonlinear) response of buildings, a large number of improved pushover procedures have been developed the last two decades. These procedures use either an invariable loading vector or a variable one, usually consisting of monotonically increasing floor forces and torques (Forced-based procedures) but in some cases also of floor enforced displacements (Direct Displacement-based procedures). The first category includes the multi-mode procedures [13-19], pushover procedures combined with some kind of linear dynamic analysis [20-23] and pushover procedures that use dynamic or corrective eccentricities in order to apply the floor lateral loads [4-7,9,12,24-25]. The adaptive pushover procedures [26-31] belong to the second category. The effectiveness of the improved pushover procedures on the seismic assessment of buildings is discussed in several published research papers [32-39]. The computational cost and the complexity of implementing some of the improved pushover procedures is another important issue to emphasize, as simplicity and clearness are key points in order to have a useful tool for the assessment of the seismic capacity of structures.

To provide a comprehensive treatment of all the previously mentioned weaknesses of the code-proposed pushover procedure on multi-storey reinforced concrete (r/c) buildings, a simple Direct Displacement-based pushover procedure has been recently proposed by Makarios and Bakalis [10-11], Bakalis and Makarios [8]. According to this procedure, three seismic enforced-displacements are applied at each floor-diaphragm with respect to an ideal inelastic principal reference system of the multi-storey r/c building: two floor enforced-translations and one floor-enforced rotation. These seismic, drift-based, floor enforced-displacements are the outcome of a large parametric analysis on multi-storey r/c buildings and aim directly at the seismic performance level of Near Collapse (NC). Using all possible sign combinations of the three floor enforced displacements, eight final pushover analyses are performed along each main loading direction and the envelope of a total of sixteen analyses provides an accurate prediction of the seismic demand, especially as regards the distribution in-plan and in-elevation of the seismic interstorey drift ratios. Key point of the process is the definition of an ideal inelastic principal reference system of the multi-storey r/c building CR_{sec} (I_{sec}, II_{sec}, III_{sec}) at the Near Collapse state, by considering that all the structural members have developed plastic hinges at their two ends. This reference system is called as "Capable Near Collapse Principal System of the multi-storey r/c building". Also, the torsional sensitivity of the multi-storey r/c building is examined relative to this ideal principal system using an enchased formula. The proposed pushover procedure can be used for the seismic assessment of any asymmetric, torsionally flexible or not, ductile, multi-storey r/c building. Regularity in elevation of the building and the formation of whatever type of plastic mechanism (except the mechanism of soft-storey) are the mandatory conditions to apply the procedure. A possible practical implementation of the proposed pushover procedure into codification could concern the safe estimation of the seismic demands of asymmetric r/c buildings at the Near Collapse state, especially of the interstorey drift ratios at the stiff sides of torsionally flexible buildings.

It is noted that, the effectiveness of the proposed

pushover procedure with enforced displacements has been fully verified in the first author's doctoral dissertation [40]. Various regular in elevation, ductile, multistorey r/c buildings were examined there, with varying number of floors, structural type, static eccentricity, and torsional sensitivity. In this paper, the effectiveness of the proposed procedure is verified by the seismic assessment of an asymmetric, torsionally flexible, six-storey r/c building using the nonlinear response history analysis.

2. Application steps of the enforced-displacement pushover procedure

The basic steps for the application of the enforced-displacement pushover procedure are summarized here. It is noted that the proposed procedure follows the rationale of Eurocode EN 1998-3 on the secant stiffness at yield of structural r/c elements (EI_{sec}), to properly simulate the extreme capable Near Collapse state of the building. Full details of the proposed methodology can be found in References [8,10,11,40].

2.1 End-section analysis of r/c elements

Given the geometry and reinforcement details of the end-sections of all structural elements, section analysis provides the Moment-Curvature (M-φ) diagrams which are then bilinearized to extract the yield moment M_y of each end-section. These diagrams are converted to Moment-Chord Rotation (M-θ) diagrams by using the plastic hinge length L_{pl} proposed in the Informational Annex A of EN 1998-3 (Eqs. (A.4) and (A.9)). In addition, Eqs. (A.10) or (A.11) in the same Annex of EN 1998-3 can be used for the calculation of the chord rotation at yield θ_y.

2.2 Secant stiffness at yield of r/c elements

The secant stiffness at yield of the end-sections of each structural element is calculated according to EN 1998-3 (Informational Annex A.3.2.4(5)):

$$EI_{sec} = M_y \cdot L_v / 3\theta_y \qquad (1)$$

where M_y and θ_y are respectively the yield moment and the chord rotation at yield calculated in the previous step and L_v is the shear span, usually taken equal to half the clear length of the structural elements. The secant stiffness at yield to be assigned to each structural member of the non-linear model of the building is the average of the corresponding stiffness of their two end-sections for negative and positive bending.

2.3 Non-linear model. Definition of an ideal inelastic principal reference system of the multi-storey r/c building.

The secant stiffness at yield must be assigned to each structural member in the nonlinear model of the r/c building. This is mandatory in EN 1998-3 [41] for the verification in terms of deformations. The same rationale is adopted by the proposed procedure. This implies the formation of plastic hinges at both end-sections of all the structural members of the building model. But this is an ideal state, characterized by the authors as the extreme Capable Near Collapse state. By considering this state of full plastic mechanism at NC, the verification of the building is always on the safe side, because the building is more flexible, and the displacements and deformations are slightly enlarged at the NC state. To simulate the locations of all possible plastic deformations in the nonlinear model, concentrated plastic hinges should be inserted at the critical end-sections of each structural member.

In the previously formed non-linear model, the following must be determined: (a) the inelastic Centre of Stiffness (CR_{sec}) of the multistorey r/c building and, hence, the in-plan location of the inelastic vertical Principal Axis (III_{sec}) passing through it, (b) the inelastic horizontal Principal Axes (I_{sec}, II_{sec}) of the multistorey r/c building, (c) the inelastic Torsional radii ($r_{I,sec}$, $r_{II,sec}$) of the multistorey r/c building. All the previously mentioned can be determined by performing a set of linear analyses, using the well-known methodology for the identification of the vertical fictitious elastic axis (torsional optimum axis) of the multi-storey building [42-52]. CR_{sec} is the pole of rotation into the floor-diaphragm closest to the height of $0.8H_{tot}$, where H_{tot} is the total building height. Thus, the above methodology approximately defines an inelastic, ideal, 3D Principal Reference System $CR_{sec}(I_{sec}, II_{sec}, III_{sec})$ for the application of non-linear methods of analysis aiming at the NC state, which is the "Capable Near Collapse Principal System of the multi-storey r/c building" so named by the authors. The term *inelastic* was selected because of the non-linear characteristics (M_y, θ_y) used in the calculation of the secant stiffness at yield (Eq. 1). Therefore, all the above inelastic properties of the multi-storey r/c building are strength dependent. The inelastic static eccentricity of the multi-storey r/c building along the I_{sec} or II_{sec} axis is equal

to the distance along the same direction between the location of the center of mass CM in each floor and that of the vertical Principal axis III_{sec}. The two main loading directions coincide with the directions of the horizontal Principal Axes I_{sec} and II_{sec}.

The (mean) torsional sensitivity of the multi-storey r/c building is verified by the following equation:

$$r_{I,sec} \text{ or } r_{II,sec} \leqslant 1.10 \cdot r_m \qquad (2)$$

where $r_m = \sqrt{J_m / m}$ is the radius of gyration of the floor closest to the $0.8H_{tot}$ level, J_m is the mass moment of inertia of the same floor about a vertical axis passing through its geometric centre and m is its mass. If the equation is fulfilled, then the multi-storey building is characterized as torsionally flexible. In the above equation, a higher limit value of 1.10 was adopted [5,8], compared to the value of 1 used in the linear area [53], to take account of the increased torsional sensitivity observed in several cases of single-story buildings in the non-linear area, initially characterized as torsionally stiff (in the linear area).

2.4 Proposed vectors of floor enforced-displacements
Figures 1 and 2 illustrate the proposed patterns in elevation of the seismic enforced interstorey drift ratios $\gamma_{I;II}$ and of the seismic floor enforced-rotations $\psi_{R,III}$ used in the framework of the proposed procedure for the verification of the building at the performance level of NC. These enforced displacements are the outcome of a large parametric analysis in various regular in elevation, ductile, multi-storey r/c buildings designed according to EN 1998-1 for Ductility Class High, by performing nonlinear response history analysis

(N-LRHA) and always considering the influence of P-Delta effects. The parameters examined were the structure type (as defined in EN 1998-1 [3]), the number of floors, the inelastic statistic eccentricity and the torsional sensitivity. The proposed values of Figures 1 and 2 are mean values determined through a statistical processing.

In Figures 1 and 2, H_i/H_n is the relative height of the examined level (H_i, measured from the ground level) to the total building height H_n. Linear interpolation can be performed for intermediate number of stories. The parameters used in Figure 1 are the structural type and the number of stories. In Figure 2, the torsional sensitivity is an additional parameter (TF for torsionally flexible buildings and TS for torsionally stiff buildings). Figures 1 and 2 provide proposed patterns of $\gamma_{I;II}$ and $\psi_{R,III}$ along each horizontal direction I_{sec} and II_{sec}, separately. Then, the unique values of the i-floor enforced-rotations $\psi_{R,III,i}$ are obtained as the average of the corresponding values along each horizontal direction. The proposed values of seismic enforced interstorey drift ratios $\gamma_{I;II}$ (rad) in elevation are converted to floor enforced translational displacements $\psi_{I;II}$ using the following equations:

$$\psi_{I;II,1} = \gamma_{I;II,1} \cdot H_1 \qquad i = 1 \qquad (3a)$$

$$\psi_{I;II,i} = \gamma_{I;II,i} \cdot H_i + \psi_{i-1} \qquad i = 2,\ldots,n \qquad (3b)$$

where H is the floor height. It is noted that the value of $\gamma_{I,II,i} \cdot H_i$ gives directly the i-floor seismic drift along the horizontal direction I_{sec} or II_{sec}. The proposed values of floor enforced-displacements given by Eq. (3) are further adapted to the building under seismic evaluation following the procedure of the next step.
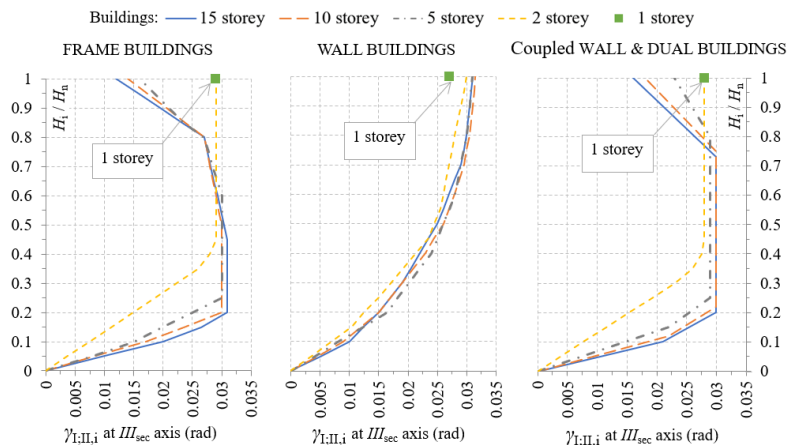

Figure 1. Proposed seismic enforced interstorey drift ratios $\gamma_{I,i}$ or $\gamma_{II,i}$ (rad) in elevation for the NC performance level, at the location of the vertical axis III_{sec} and along the horizontal directions I_{sec} and II_{sec} (all cases of inelastic static eccentricity and torsional sensitivity).

2.5 Temporary nonlinear static analyses along the ideal principal axes I_{sec} and II_{sec} of the multi-storey building

The proposed patterns of floor enforced interstorey drift ratios $\gamma_{I;II}$ can be adapted more specifically to the examined r/c multi-storey building by the envelope of two temporary sets of pushover analyses (with lateral floor forces and considering the P-Delta effects) along the horizontal directions I_{sec} and II_{sec}. In the first set of pushover analyses (2 analyses along the I_{sec} axis and more 2 analyses along the II_{sec} axis, considering the two signs ($\pm$) of application of the floor lateral forces), the floor lateral forces are applied at the location of the vertical III_{sec} axis having a pattern according to the first uncoupled fundamental translational mode along each horizontal ideal direction, I_{sec} or II_{sec}.
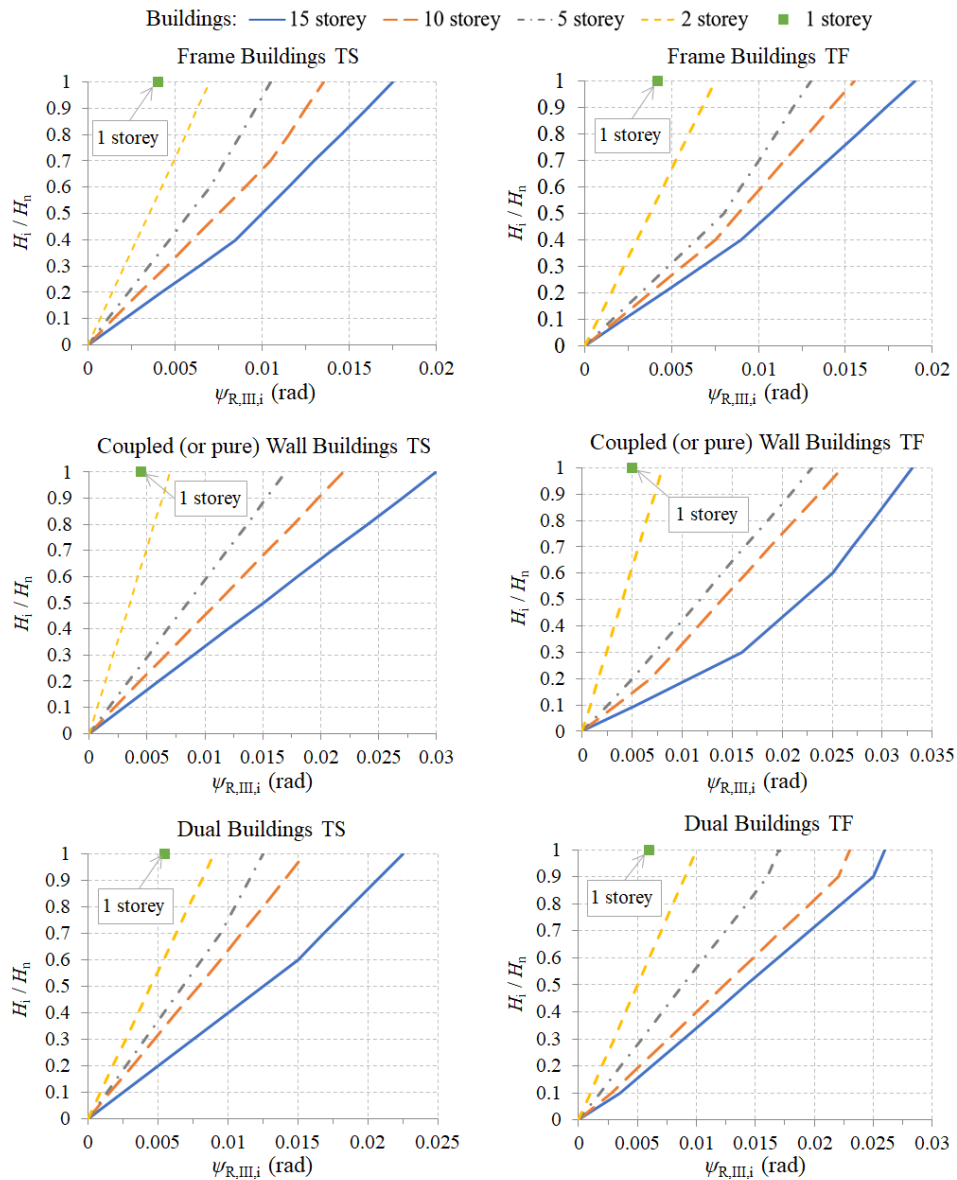
Figure 2. Proposed seismic floor enforced-rotations $\psi_{R,III,i}$ (rad) about vertical axis in elevation for the NC performance level (all cases of inelastic static eccentricity)

The second set of pushover analyses is similar to the first (2 analyses along the I_{sec} axis and 2 analyses along the II_{sec} axis, considering the two signs ($\pm$) of application of the floor lateral forces) with the difference that only the 80% of the base shear is used, while the remainder 20% of the base shear is applied as a concentrated lateral load at the top of the vertical III_{sec} axis. In both sets, the value of the base shear that is

distributed in elevation can be considered equal to one (unit base shear). The target displacement of the two temporary sets of pushovers can be obtained from Table 1. This Table contains the results of a large parametric analysis on multi-storey r/c buildings about the mean value of the seismic drift ratio $\gamma_{t,top}$ of the building top at the location of the vertical III_{sec} axis, along the directions of the I_{sec} and II_{sec} axes. For intermediate structural types of dual systems (consisting of frames and walls) or coupled (via beams) wall systems, as well as for various number of storeys, linear interpolation is performed. These values are valid for all cases of inelastic static eccentricity and torsional sensitivity. The final values of the proposed interstorey drift ratios,

which will be used to calculate the floor enforced translational displacements of the proposed procedure along the I_{sec} and II_{sec} axes (Eq.3), are calculated as the average of the proposed values of Figure 1 and of those computed from the envelope of the two temporary sets of pushover analyses [40]. It should be noted that, in [8], the envelope of the $\gamma_{I,II}$ values from the three previous sources was initially proposed for the safe calculation of the enforced translational displacements. However, the difference is small and in the first author's doctoral dissertation the average values were preferred, mainly for the most efficient adjustment of the $\gamma_{I,II}$ values at the lower floors of multi-storey r/c buildings.

Table 1. Mean seismic (target) drift ratio $\gamma_{t,top}$ (rad) of the building at the NC state, on the top of the vertical ideal axis III_{sec} and along the horizontal ideal principal axes I_{sec} and II_{sec}.

Number of Storeys	1	2	5	10	15
Pure frame buildings without walls	0.0300	0.0295	0.0235	0.0205	0.0195
Pure wall buildings without frames	0.0280	0.0290	0.0260	0.0240	0.0230

2.6 Enforced-displacement combinations to consider the spatial action of the earthquake

To consider the spatial character of the seismic action, the three enforced-displacements $\psi_{I,i}$, $\psi_{II,i}$ and $\psi_{R,III,i}$ should act simultaneously on the location of the vertical III_{sec} axis inside each i-floor but with an appropriate way along each main loading direction I_{sec} and II_{sec}. Therefore, the floor enforced translational displacement along the examined (main) loading direction keep its full value inside the combinations while the second floor enforced translational displacement, along the other (normal) direction, is inserted in the combinations with 30% of its full value. Considering the two signs (±) of action of the floor enforced-displacements, eight possible combinations of them are obtained for each one of the main loading directions I_{sec} and II_{sec}. These combinations are presented in Tables 2 and 3, in which

the ""+" " or "-" symbol indicates with emphasis the combined values of seismic enforced-displacements.

2.7 Estimation of the seismic demand

The sixteen final pushover analyses of Tables 2 and 3 are performed using as target displacement the value of the enforced translational displacement at the top of the vertical axis III_{sec}, along each main loading direction I_{sec} and II_{sec}. Therefore, the target displacement is equal to the value $\psi_{I,II,n}$ calculated by Eq. (3b), where n is the top floor. The envelope of the response of the sixteen pushover analyses of the proposed procedure provides a safe prediction of the seismic demand at the NC state, especially as regards the interstorey drift ratios. The floor displacements are computed slightly conservatively in multi-storey buildings with more than three floors and are corrected according to the next step.

Table 2. Earthquake spatial action of simultaneous floor enforced-displacements that maximize the displacement along I_{sec} axis

Eight (8) enforced-displacement combinations of nonlinear static analysis	
"+"$\psi_{I,i}$"+" $0.3 \cdot \psi_{II,i}$"+" $\psi_{R,III,i}$	"+"$\psi_{I,i}$"+" $0.3 \cdot \psi_{II,i}$"−" $\psi_{R,III,i}$
"+"$\psi_{I,i}$"−" $0.3 \cdot \psi_{II,i}$"+" $\psi_{R,III,i}$	"+"$\psi_{I,i}$"−" $0.3 \cdot \psi_{II,i}$"−" $\psi_{R,III,i}$
"−"$\psi_{I,i}$"+" $0.3 \cdot \psi_{II,i}$"+" $\psi_{R,III,i}$	"−"$\psi_{I,i}$"+" $0.3 \cdot \psi_{II,i}$"−" $\psi_{R,III,i}$
"−"$\psi_{I,i}$"−" $0.3 \cdot \psi_{II,i}$"+" $\psi_{R,III,i}$	"−"$\psi_{I,i}$"−" $0.3 \cdot \psi_{II,i}$"−" $\psi_{R,III,i}$

Table 3. Earthquake spatial action of simultaneous floor enforced-displacements that maximize the displacement along II_{sec} axis

Eight (8) enforced-displacement combinations of nonlinear static analysis	
$"+"0.3{\cdot}\psi_{I,i}"+"\ \psi_{II,i}"+"\ \psi_{R,III,i}$	$"+"0.3{\cdot}\psi_{I,i}"+"\ \psi_{II,i}"-"\ \psi_{R,III,i}$
$"+"0.3{\cdot}\psi_{I,i}"-"\ \psi_{II,i}"+"\ \psi_{R,III,i}$	$"+"0.3{\cdot}\psi_{I,i}"-"\ \psi_{II,i}"-"\ \psi_{R,III,i}$
$"-"0.3{\cdot}\psi_{I,i}"+"\ \psi_{II,i}"+"\ \psi_{R,III,i}$	$"-"0.3{\cdot}\psi_{I,i}"+"\ \psi_{II,i}"-"\ \psi_{R,III,i}$
$"-"0.3{\cdot}\psi_{I,i}"-"\ \psi_{II,i}"+"\ \psi_{R,III,i}$	$"-"0.3{\cdot}\psi_{I,i}"-"\ \psi_{II,i}"-"\ \psi_{R,III,i}$

2.8 Correction of the floor displacement profiles

Since the goal of the proposed pushover procedure with floor enforced-displacements is to capture the maximum interstorey drift ratios of each floor-diaphragm, the estimates for the floor seismic displacement profiles will be slightly conservative, especially from the middle height of a multi-storey building to its top [1]. The abovementioned issue can be observed in multi-storey buildings with more than three floors. This is inevitable, since the floor enforced-displacements $\psi_{I,II}$ are calculated sequentially with Eq. (3), from the base of the building to its top, through the proposed interstorey drift ratios $\gamma_{I,II}$ which estimated conservatively in the parametric analysis with N-LRHA and express the maximum seismic interstorey drift ratios observed in the different floors of the building. However, these maximum values of interstorey drift ratios do not occur simultaneously.

To correct this conservatism, the values of $\gamma_{t,top}$ in Table 1 can be used as a weighting factor on the value of the enforced translational displacement $\psi_{I,II,n}$ at the top of the building calculated by Eq. (3). Therefore, the following reduction factor S_u is proposed to apply totally on the floor displacement profiles along the I_{sec} and II_{sec} axes [40]:

$$S_u = \frac{\gamma_{t,top} \cdot H_n}{\psi_n} \qquad (4)$$

where H_n is the total height of the building, $\gamma_{t,top}$ is taken from Table 1 and ψ_n is calculated by Eq. (3). The use of the reduction factor S_u is proposed for multi-storey buildings with four or more floors. The decrease shown on the floor displacement profiles by this factor is about 7-15%, where the largest values apply to high-rise buildings.

3. Numerical example of a 6-storey dual building

3.1 Building characteristics

The six-storey r/c building shown in Figure 3 is examined to verify the proposed pushover procedure on torsionally flexible multi-storey buildings. The construction materials are concrete C25/30 and steel B500c with mean strengths f_{cm} = 33 MPa and f_{ym} = 550 MPa, respectively. The building has a polygonal plan shape consisting of perimetric and interior frames and of perimetric walls. A 15 cm thick rigid floor-diaphragm is extended outside the perimeter of the floor plan forming a continuous cantilever 1 m wide. The cross-sections of all the structural elements do not change in elevation. Each floor has 3.5 m height, giving a total building height of 21 m. The six-storey building is regular in elevation but asymmetric in-plan, mainly due to the placement of walls at the building perimeter (two walls along x and y directions and a skew one). The x and y walls have rectangular cross-sections of dimensions 1.5/0.3 m and 0.3/1.8 m while the skew one has a rectangular section 1.5/0.3 m having a barbell at one end of dimension 0.5/0.5 m. All the columns are square of dimensions 0.5/0.5 m. The beams have a T-section of dimensions 30/60/150/15, where the effective flange width is considered different in linear and nonlinear analysis (1.5 m in nonlinear analysis and according to EN 1998-1 and EN 1992-1 [54] in linear analysis). The mean gravitational distributed load on all floors -including self-weights and masonry- (dead G + live Q) is about 12 kN/m², giving a translational mass of 450 tn and a mass moment of inertia about vertical axis of 34000 tn·m² for each floor. The latter is artificially increased to 60000 tn·m² in each floor, in order to have a torsionally flexible building (on limit).

3.2 Building design

The building is designed according to the provisions of EN 1992-1 and EN 1998-1 for Ductility Class High (DCH). Modal response spectrum analysis was performed in the linear building model with PGA = 0.24g (where g is the gravity acceleration), soil category D and total behavior factor q = 4.
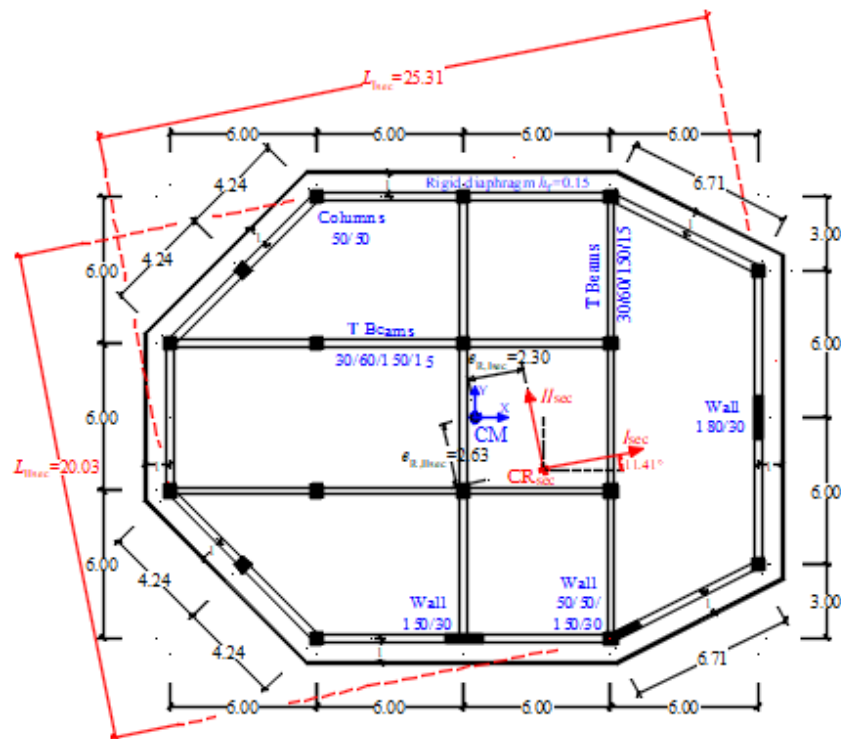
Figure 3. Nonlinear model of the six-storey r/c building

All the structural members of the linear model have been provided with their effective flexural and shear stiffness, equal to one-half of their respective geometric stiffness. The building is classified into the structural type of dual buildings, equivalent to frame buildings according to EN1998-1, along both the horizontal ideal principal axes I_{des} and II_{des}. The translational uncoupled periods of the linear model are 1.15 sec along the II_{des} axis and 1.05 sec along the I_{des} axis. The horizontal ideal principal axes I_{des} and II_{des} of the linear model are rotated relative to the x,y-axes by 14.06o counterclockwise. The two static eccentricities $e_{I,des}$ and $e_{II,des}$ along the I_{des} and II_{des} axes (distance between CR_{des} and CM in the floor-diaphragm closest to the $0.8H_{tot}$ level (fifth floor) from the base) are about equal to $0.06 \cdot L_{I,des}$ and $-0.13 \cdot L_{II,des}$ respectively, where $L_{I,des}$ and $L_{II,des}$ are the maximum plan dimensions along the two horizontal principal axes. Additionally, the building is characterized as torsionally flexible since the (mean) normalized torsional radii $r_{II,des}/r_m = 0.96$ is less than 1 (the other ratio $r_{I,des}/r_m$ is equal to 1.06), where $r_m = 11.55$ *m* is the radius of gyration of the floor-mass at the fifth floor. The as designed building has appropriate longitudinal/confinement steel reinforcement details that provide an overall high ductile behavior, spreading

the ductility demands to the end-sections of all beams and to the base end-sections of all columns/walls (beam-sway mechanism). The numbering of the structural members in the mathematical model of the building, the dimensions of the cross-sections and the reinforcement details are presented in Figure A1 and in Tables A1–A3 of Appendix A.

3.3 Non-linear model of the building

Section analysis is performed by the module Section Designer of the FEM program SAP2000 [55] which is used as the analysis tool. Having the M-φ curves along the local axes of the end-sections of all the structural members, as well as their shear span L_v and the plastic hinge length L_{pl} by the Eq. (A9) of EN 1998-3 (with γ_{el} coefficient equal to 1.7), we can obtain the respective M-θ curves and subsequently calculate the secant stiffness at yield EI_{sec} of all the structural members of the nonlinear building model (Eq. (1)). The mean values in elevation of the ratio EI_{sec}/EI_g for each type of structural member of the nonlinear model are shown in Table 4, where EI_g is the geometric stiffness. These values vary along the two local axes of columns and walls (2 and 3 axes) due to the different shear span L_v in four columns with cantilever bending mode and due to the different strength M_y and shear span L_v along

the strong (axis 3) and weak (axis 2) directions of walls. We can observe the low values of the members' bending stiffness, especially those of beams. These EI_{sec} values are assigned to all the structural members of the nonlinear building model.

The "Capable Near Collapse Principal System, $III_{sec}(CR_{sec})$, I_{sec}, II_{sec}" of the six-story r/c building is next determined according to Section 2, at the floor-diaphragm closest to the level $0.8H_{tot} = 16.8$ m from the building base, i.e., at the fifth floor with height equal to 17.5 m from the ground. Figure 3 shows the in-plan location of the inelastic center of stiffness CR_{sec} and the orientation of the horizontal ideal inelastic principal axes I_{sec}, II_{sec} in the nonlinear building model.

Table 4. Mean values in elevation of the ratio of the secant stiffness at yield to the geometric stiffness, EI_{sec}/EI_g

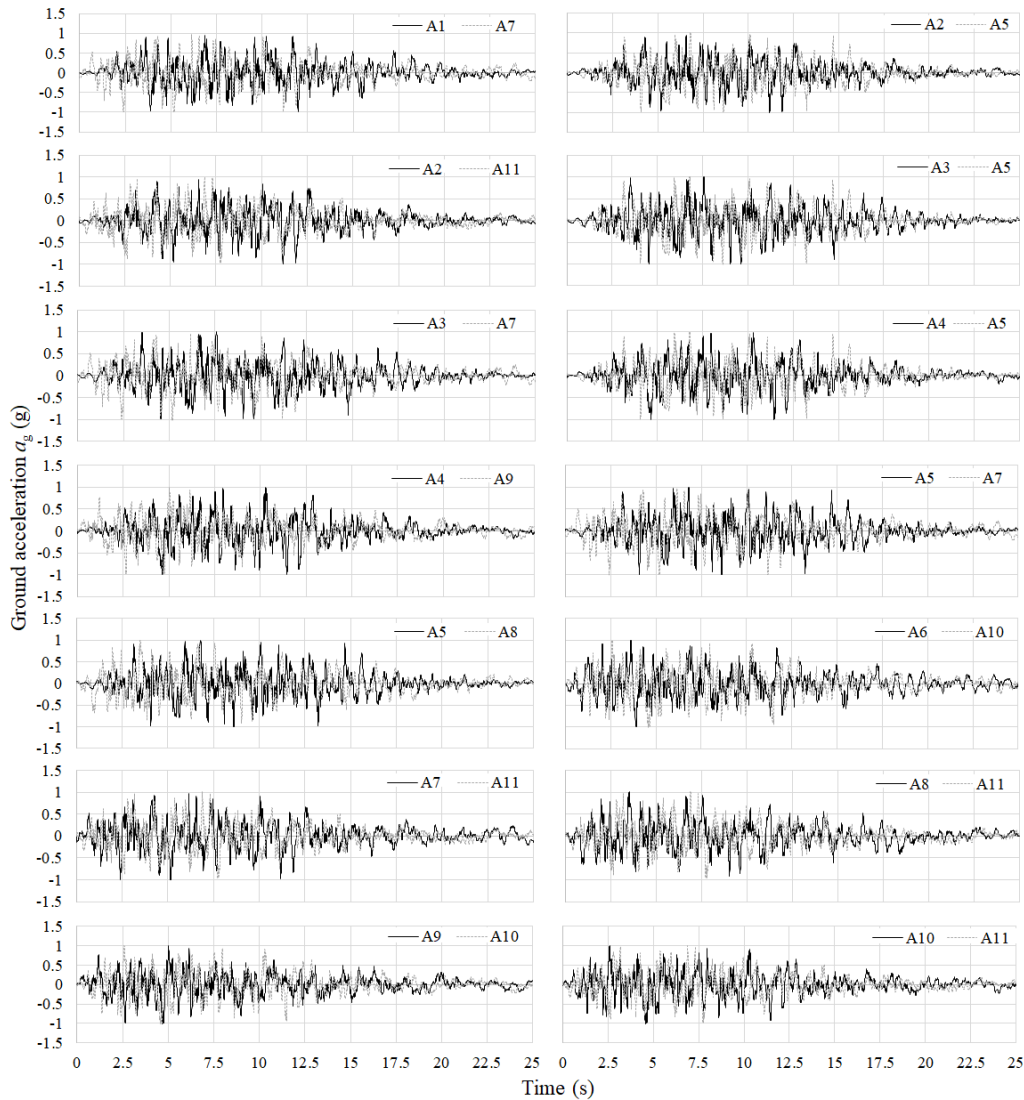| storey	Columns		Walls		Beams
	Local 3	Local 2	Local 3	Local 2	Local 3
1	0.16	0.19	0.30	0.21	0.105
2	0.15	0.19	0.27	0.20	0.110
3	0.15	0.18	0.20	0.15	0.110
4	0.12	0.13	0.16	0.13	0.095
5	0.11	0.12	0.11	0.10	0.085
6	0.10	0.10	0.07	0.08	0.075

Figure 4. 14 pairs of unit-normalized artificial accelerograms

The latter are turned relative to the x, y-axes by 11.5° counterclockwise. The inelastic static eccentricities are equal to $e_{R,Isec} = 2.3$ m and $e_{R,IIsec} = 2.63$ m and their normalized values are equal to $e_{R,Isec}/L_{Isec} = 0.09$ and $e_{R,IIsec}/L_{IIsec} = -0.13$, where L_{Isec} and L_{IIsec} are the maximum plan dimensions along the axes I_{sec} and II_{sec}, respectively. The (mean) normalized inelastic torsional radii are equal to $r_{IIsec}/r_m = 0.95$ and $r_{Isec}/r_m = 1.06$, where $r_m = 11.55$ m is the radius of gyration of the floor-mass at the fifth floor. Therefore, the nonlinear building model is characterized as torsionally flexible according to Eq. (2), because the smaller of the two torsional radii ratios (0.95) is lower than 1.10. We come to the same conclusion by examining the uncoupled fundamental modes of the non-linear model, with periods of $T_{IIsec} = 2.23$ sec, $T_{Isec} = 2.00$ sec for the translational ones and $T_{R,IIIsec} = 2.11$ sec for the torsional one. In Table 5, the periods and the modal participating mass ratios of the first nine mode-shapes of the nonlinear model of the building are presented. Additionally, the building is classified according to EN1998-1 into the structural type of dual buildings, equivalent to wall buildings along the horizontal axis I_{sec} and to frame buildings along the other horizontal axis II_{sec}. This difference in structural classification along the I_{sec} between the nonlinear (dual equivalent to wall buildings) and linear (dual equivalent to frame buildings) building models is mainly due to the greater reduction of the lateral stiffness of the frames relative to that of the walls because of the consideration of the secant stiffness at yield (Table 4).

Finally, point hinges of type M_3 (pure bending) and P-M_2-M_3 (biaxial bending with axial force) are inserted at the end-sections of each beam and column/wall of the nonlinear model, respectively, with constitutive laws according to Mander *et al*. [56] for the unconfined/confined concrete and according to Park and Paulay [57] for the steel reinforcement. The backbone curves of the response of the fiber hinges at the end-sections of the structural elements (determined from the abovementioned constitutive laws) and the Takeda and the Kinematic hysteresis model for the concrete and the steel rebars respectively are embedded in the SAP2000 FEM program used for the nonlinear analysis. Additional information can be found in SAP2000 analysis manual.

It is noted that accidental eccentricity was not considered in nonlinear analysis. As was observed in the extended parametric analysis of regular in elevation, ductile, asymmetric, r/c multi-storey buildings implemented in the doctoral dissertation of the first author [40], the value of the accidental eccentricity proposed by the seismic codes has only a very minor impact on the nonlinear response in the deep nonlinear area (Near Collapse).

Table 5. Periods and participating mass ratios of uncoupled and coupled modes of the nonlinear building model

Uncoupled Mode	Period (sec)	UX	UY	RZ	Coupled Mode	Period (sec)	UX	UY	RZ
1	2.233	0.030	0.753	0.002	1	2.478	0.062	0.441	0.309
2	2.109	0.006	0.000	0.786	2	2.132	0.461	0.238	0.086
3	1.998	0.745	0.030	0.002	3	1.782	0.261	0.108	0.385
4	0.726	0.002	0.082	0.024	4	0.832	0.011	0.050	0.045
5	0.697	0.031	0.016	0.065	5	0.699	0.069	0.039	0.006
6	0.645	0.083	0.017	0.024	6	0.562	0.035	0.025	0.065
7	0.404	0.001	0.017	0.023	7	0.469	0.005	0.017	0.019
8	0.376	0.023	0.020	0.006	8	0.375	0.029	0.018	0.001
9	0.324	0.025	0.013	0.018	9	0.312	0.004	0.010	0.008

3.4 Seismic demand

The inertial characteristics of the nonlinear model of the six-storey building are concentrated at the geometric centre of each i-floor ($m_i = 450$ tn, $J_{m,i} = 60000$ tn·m²). Figure 4 shows the 14 pairs of uncorrelated artificial accelerograms -formed by 11 unit-normalized accelerograms of 25 sec duration- which are used for the nonlinear response history analysis (N-LRHA) of the six-storey building, to provide the seismic demand. The artificial accelerograms were constructed by SeismoArtif [58] aiming to fit as close as possible (±10%) the unit PGA, 5% damped, design elastic

acceleration spectrum of EN 1998-1 for soil category *D* (Figure 5). The significant (strong motion) duration of the accelerograms is about 14-18 sec and the Arias Intensity is 28 m/s on average, characteristics like those of the Hellenic tectonic faults [59]. The characteristics of the 11 unit-normalized artificial accelerograms are shown in Table 6, as reported by SeismoArtif. Next, the two seismic components of each pair are scaled to PGA = 0.4*g* during analysis in order the building to attain the Near Collapse state. Additionally, each pair is rotated successively per 15° in order to find the worst seismic load scenario [47] by the 24 analyses obtained for each pair. Also, the four sign (±) combinations of the two seismic components of each pair were examined. The envelope of the response of 14 x 24 x 4 = 1344 N-LRHA is considered as the seismic demand, at every control location, to compare with the response effects of the proposed pushover procedure at the Near Collapse (NC) state. The average response from the N-LRHA is also recorded.
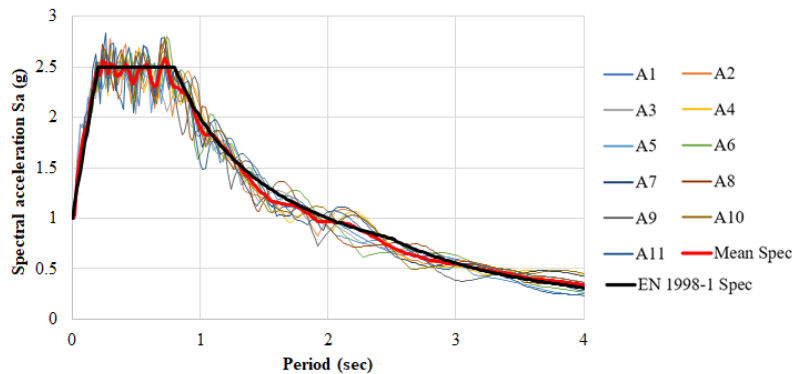

Figure 5. Mean spectrum of artificial accelerograms vs EN 1998-1 design elastic spectrum
($\xi = 0.05$, PGA = 0.4*g*, soil *D*)

Table 6. Artificial accelerogram characteristics

Accelerogram	A1	A2	A3	A4	A5	A6	A7	A8	A9	A10	A11
Max Acceleration (g)	0.99	1.00	1.00	1.00	1.00	0.99	1.00	1.00	1.00	1.00	1.00
Max Velocity (cm/sec)	241.85	151.42	179.28	149.63	162.71	156.34	191.53	221.30	184.26	178.82	188.13
Max Displacement (cm)	384.42	54.71	75.47	140.46	65.88	75.65	126.50	480.58	187.09	166.50	192.27
Vmax/Amax (sec)	0.25	0.15	0.18	0.15	0.17	0.16	0.19	0.23	0.19	0.18	0.19
Acceleration RMS (g)	0.27	0.26	0.27	0.26	0.28	0.27	0.28	0.27	0.25	0.27	0.25
Velocity RMS (cm/sec)	77.00	40.54	40.63	48.44	38.11	42.28	47.47	87.01	58.57	54.89	50.95
Displacement RMS (cm)	166.57	17.61	23.55	63.49	23.07	29.74	61.28	239.80	113.63	77.57	92.26
Arias Intensity (m/sec)	29.03	26.03	28.74	26.66	29.23	28.31	29.19	27.39	24.46	28.38	24.42
Characteristic Intensity	0.72	0.66	0.71	0.67	0.72	0.71	0.72	0.69	0.63	0.71	0.63
Specific Energy Density (cm2/sec)	148285	41107	41277	58686	36315	44707	56346	189336	85781	75357	64929
Cum. Abs. Velocity (cm/sec)	4743.6	4405.2	4666.4	4348.7	4642.8	4951.	4915.3	4718.9	4501.6	4716.0	4389.4
Acc Spectrum Intensity (g*sec)	0.96	0.95	0.95	0.94	0.95	0.96	0.95	0.96	0.96	0.96	0.95
Vel Spectrum Intensity (cm)	654.10	659.10	646.44	653.68	644.19	636.91	662.37	628.21	648.40	643.51	661.66
Housner Intensity (cm)	629.25	634.98	611.72	637.95	614.88	623.84	641.22	616.83	639.60	643.14	636.73
Sustained Max.Acceleration (g)	0.93	0.95	0.99	0.98	0.97	0.92	0.98	0.92	0.99	0.93	0.96
Sustained Max.Velocity (cm/sec)	178.42	121.72	110.04	139.51	114.05	132.98	124.22	170.09	162.42	144.99	115.79
Effective Design Acceleration (g)	0.93	0.95	1.02	0.99	1.03	0.99	1.01	0.94	1.02	0.97	1.00
A95 parameter (g)	0.95	0.99	0.98	0.98	0.98	0.98	0.98	0.98	0.99	0.99	0.99
Predominant Period (sec)	0.56	0.30	0.24	0.30	0.58	0.74	0.72	0.24	0.72	0.72	0.26
Significant Duration (sec)	14.93	14.14	14.93	14.17	14.11	18.05	17.30	17.28	17.24	16.15	14.64

3.5 Proposed interstorey drift ratios and floor enforced-rotations

For the implementation of the proposed procedure of pushover analysis, the initially proposed interstorey drift ratios $\gamma_{I,i}$, $\gamma_{II,i}$ at the in-plan location of the vertical axis III_{sec} are obtained from Figure 1 for dual buildings along both the axes I_{sec} and II_{sec}. Also, the proposed floor enforced-rotations $\psi_{R,III,i}$ are obtained from Figure 2 for dual torsional flexible buildings along both the axes I_{sec} and II_{sec}. These proposed values of enforced-displacements are presented in Figure 6. The initial values of the proposed interstorey drift ratios will be reviewed through the methodology described in the next step.
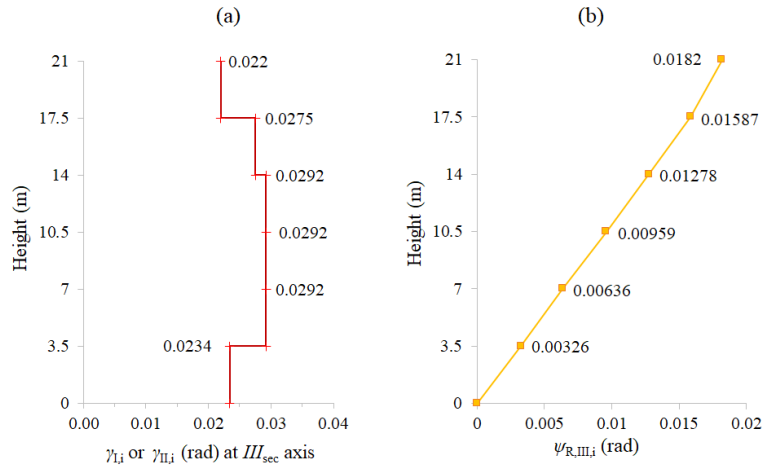

Figure 6. Proposed values of (a) interstorey drift ratios $\gamma_{I;II}$ (rad) and (b) floor enforced-rotations $\psi_{R,III}$ (rad)

3.6 Two temporary sets of pushover analysis to calculate the final proposed floor enforced translations

Two temporary sets of pushover analysis (with forces) are performed to find revised values of interstorey drift ratios $\gamma_{I,i}$, $\gamma_{II,i}$. The pattern of floor lateral forces in the two sets, which are applied at the in-plan location of the vertical axis III_{sec} along the ($\pm$) directions of the horizontal I_{sec} and II_{sec} axes, is depicted in Figure 7.

These floor forces correspond to a unit base shear that is distributed in elevation according to the translational building modes along the I_{sec} and II_{sec} axes in both sets but with an additional top force in the second set equal to 20% of the base shear. The target displacement at the top of the vertical axis III_{sec}, along both the I_{sec} and II_{sec} axes, is calculated directly from Table 1 by double linear interpolation for multi-storey buildings with six floors and with a dual structural system:

$$u_t = \gamma_{t,top} \cdot H_{tot} = \frac{\left(0.0235 - \dfrac{0.0235 - 0.0205}{5}\right) + \left(0.026 - \dfrac{0.026 - 0.024}{5}\right)}{2} \cdot 21.00$$
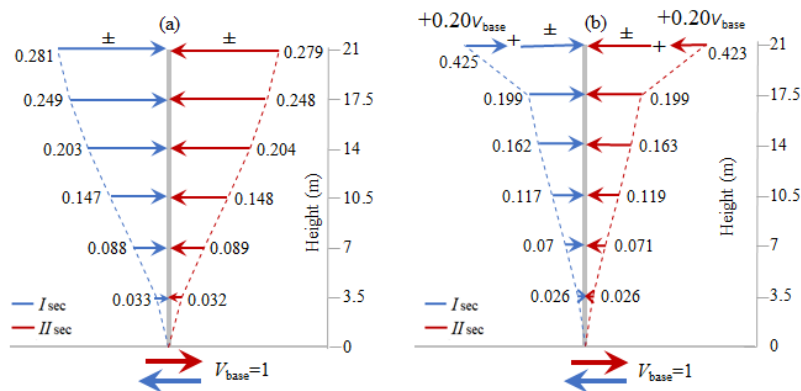
$$= 0.0245 \cdot 21.00 = 0.515\,m$$

Figure 7. Pattern of floor lateral static loads on the in-plan location of the vertical III_{sec} axis and along the horizontal I_{sec} and II_{sec} axes: (a) first temporary set of (4) pushover analyses, (b) second temporary set of (4) pushover analyses

It is noted that the envelope of the displacement results from N-LRHA provides a displacement at the top of the vertical axis III_{sec} equal to 0.574 m along both the I_{sec} and II_{sec} axes, which is greater from the previous one (the mean displacements from N-LRHA at the same point are about 0.40 m along both the horizontal principal directions). Additionally, by performing the methodology of EN 1998-1 Informational Annex B with the NC seismic action of PGA = 0.4g we get 0.54 m and 0.60 m for the corresponding displacements along the I_{sec} and II_{sec} axes.

The envelope of the interstorey drift ratios $\gamma_{I,i}$, $\gamma_{II,i}$ resulted from the eight total pushovers of the two

temporary sets is shown in the 2nd and 3rd column of Table 7. The average of these values with the corresponding ones initially proposed by Figure 1 (depicted in Figure 6 and shown in the 4th column of Table 7) are considered as the final interstorey drift ratios (5th and 6th column of Table 7) for the calculation of the floor enforced translational displacements $\psi_{I,i}$, $\psi_{II,i}$ using Eq. 3. The three enforced displacements of the proposed pushover procedure, which act at the location of the vertical III_{sec} axis inside each floor-diaphragm, are shown at the last three columns of Table 7.

Table 7. Calculation of the final floor enforced-displacements

	Interstorey drift ratios $\gamma_{I,i}$ and $\gamma_{II,i}$ (rad)					Floor enforced displacements		
	Temp. Pushovers ENV		Prop. Values, Figure 6	Final proposed values				
	Dir I_{sec}	Dir II_{sec}	Dir I_{sec} , II_{sec}	Dir I_{sec}	Dir II_{sec}	$\psi_{I,i}$ (m)	$\psi_{II,i}$ (m)	$\psi_{R,III,i}$ (rad)
1st	0.0240	0.0209	0.0234	0.0237	0.0222	0.083	0.078	0.0033
2nd	0.0328	0.0327	0.0292	0.0310	0.0309	0.191	0.186	0.0064
3rd	0.0322	0.0339	0.0292	0.0307	0.0315	0.299	0.296	0.0096
4th	0.0283	0.0293	0.0292	0.0287	0.0292	0.399	0.398	0.0128
5th	0.0233	0.0229	0.0275	0.0254	0.0252	0.488	0.487	0.0159
6th	0.0169	0.0162	0.0220	0.0194	0.0191	0.556	0.553	0.0182

3.7 Proposed pushover procedure for the estimation of the seismic demand. Verification

The sixteen pushovers of Tables 2 and 3 are performed with target displacement along the main loading directions I_{sec} and II_{sec} equal to $\psi_{I,6} = 0.556$ m and $\psi_{II,6} = 0.553$ m (Table 7). The envelope of the response from the 16 pushover analyses of the proposed pushover procedure can be considered as an estimation of the seismic demand.

The effectiveness of the proposed pushover procedure on the prediction of seismic demand will be verified against the results of N-LRHA, which is the benchmark method. Additionally, the response effects by the proposed pushover procedure compare with those resulted by the N2 [3,60] and Extended N2 pushover procedures [21]. In the latter procedure, the response effects resulted by the conventional N2 pushover adopted by EN 1998-1 are corrected, in-plan and in elevation, using corrections factors determined from the results of a 3D modal response spectrum analysis. It is noted that, in the framework of the N2 pushover the

lateral forces are applied on the location of CM inside each floor (without accidental eccentricity) along the horizontal ideal principal axes I_{sec} and II_{sec} of the six-storey building. The target displacement (at CM of the top floor) was considered equal to that resulted from N-LRHA.

The patterns of interstorey drift ratios in elevation, at the flexible and stiff sides of the building as well as at the location of CM and that of the vertical III_{sec} axis (CR$_{sec}$) inside each floor, are presented in Figure 8. The (%) errors committed on the estimation of the seismic demand (N-LRHA) by the proposed and the Extended N2 pushovers are recorded in Table 8, where the (−) sign indicates unconservative estimates. It is obvious from Figure 8 that the N2 pushover procedure seriously underestimates the interstorey drift ratios at the stiff sides of the building, all over its height. It also underestimates the interstorey drift ratios at any location in the upper half of the building.
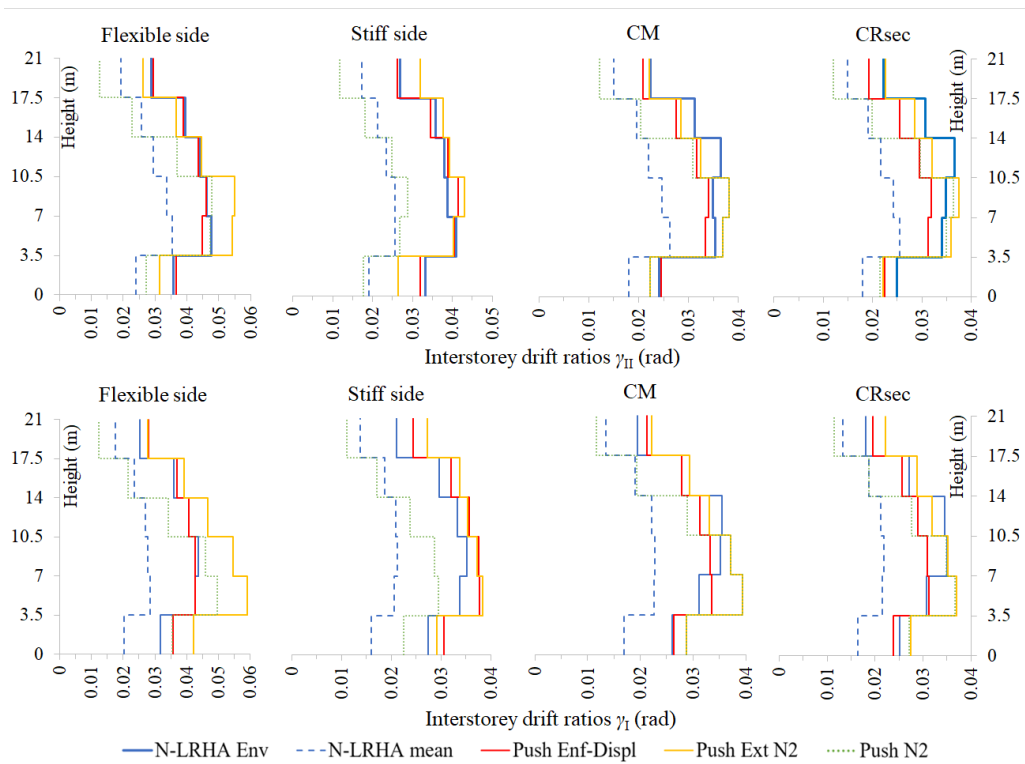
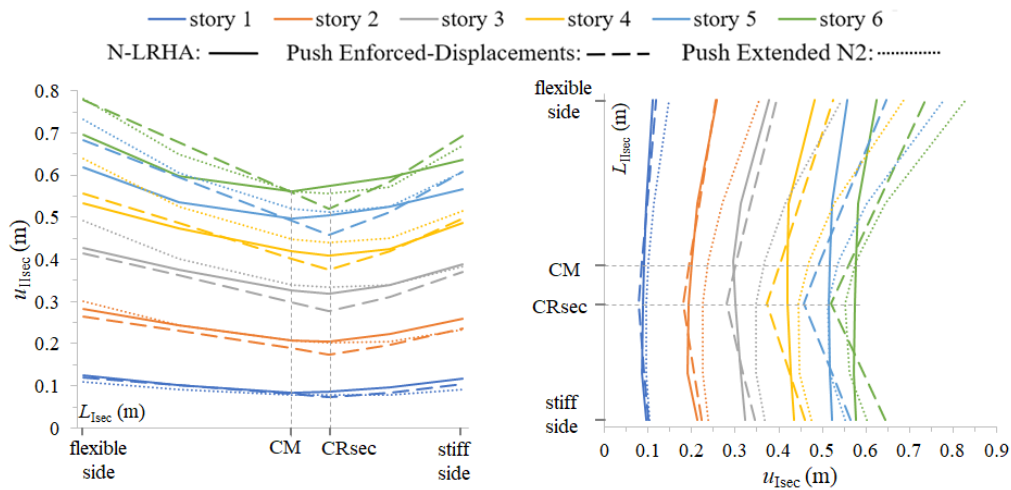**Figure 8.** Interstorey drift ratios: Proposed pushover procedure vs N-LRHA and Extended N2 pushover

Figure 9. Floor displacement profiles: Proposed pushover procedure vs N-LRHA and Extended N2 pushover

Table 8. Errors (%) on the estimation of the seismic interstorey drift ratios

	Pushover with Enforced Displacements				Pushover Extended N2			
	Direction II_{sec}							
Floor	CM	CR	Stiff Side	Flex Side	CM	CR	Stiff Side	Flex Side
1	2	−10	−3	3	−7	−11	−20	−12
2	−6	−8	−1	−6	4	6	−2	14
3	−2	−8	7	0	9	8	11	19
4	−13	−19	2	−2	−11	−12	3	1
5	−12	−17	−3	−1	−9	−7	6	−7
6	−7	−13	−2	2	−2	2	19	−9

	Pushover with Enforced Displacements				Pushover Extended N2			
				Direction I_{sec}				
Floor	CM	CR	Stiff Side	Flex Side		CM	CR	Stiff Side	Flex Side
1	1	−5	12	13		10	9	6	33
2	8	1	12	0		26	20	13	39
3	−5	−12	7	−2		6	1	6	25
4	−12	−16	7	0		−7	−8	6	14
5	0	−6	8	2		5	6	14	8
6	10	8	16	11		14	22	30	10

On the contrary, N2 pushover overestimates in general the interstorey drift ratios at any location (except the stiff sides) in the lower half of the building (2nd and 3rd floor). We can also see from Figure 8 and Table 8 that the seismic interstorey drift ratios at the flexible and stiff sides of the six-storey building are safely or marginally estimated by the proposed pushover procedure. These estimates are more balanced than those of the Extended N2 pushover, which provides in general more conservative estimates but also some unconservative ones along the II_{sec} axis at the first floor. At the in-plan location of CR$_{sec}$, the seismic interstorey drift ratios are in general slightly underestimated by the proposed procedure due to the smaller value of the target (enforced) displacements used in pushover analysis compared to the corresponding N-LRHA displacements. But at the in-plan location of CM the interstorey drift ratios are in general marginally estimated.

According to section 2, the floor displacements computed by the proposed pushover procedure must be totally reduced by the factor S_u of Eq. (4):

$$S_u = \frac{\gamma_{t,top} \cdot H_n}{\psi_6} = \frac{0.0245 \cdot 21.00}{0.553} = \frac{0.515}{0.553} = 0.931$$

where $\gamma_{t,top} \cdot H_n = 0.515$ m is the proposed top target displacement of the temporary pushovers (from Table 1) previously calculated and $\psi_{I,II,6} = 0.556$ or 0.553 m is the enforced translational displacement of the building top (Table 7). In Figure 9, the floor displacements profiles resulted by the proposed pushover procedure compare with the corresponding ones by N-LRHA and Extended N2 pushover.

Table 9. Errors (%) on the estimation of the seismic floor displacements

	Pushover with Enforced Displacements				Pushover Extended N2			
				Direction II_{sec}				
Floor	CM	CRsec	Stiff Side	Flex Side		CM	CRsec	Stiff Side	Flex Side
1	−5	−16	−10	−5		−7	−11	−20	−12
2	−9	−15	−9	−6		0	−1	−10	6
3	−8	−12	−5	−3		5	5	−1	15
4	−4	−8	2	4		7	8	6	20
5	−1	−9	7	10		5	2	7	18
6	0	−9	9	12		0	−3	5	12
				Direction I_{sec}				
Floor	CM	CRsec	Stiff Side	Flex Side		CM	CRsec	Stiff Side	Flex Side
1	−6	−12	4	5		10	9	6	33
2	−2	−7	4	−1		19	17	11	37
3	3	−7	7	5		25	16	14	45
4	−3	−11	6	9		12	6	9	43
5	−4	−11	8	16		4	−1	6	40
6	−2	−9	12	18		0	−4	5	33

The (%) errors committed on the estimation of the seismic demand are recorded in Table 9. We observe that, at the in-plan location of the vertical III_{sec} axis (CR_{sec}) the floor displacements are slightly underestimated by the proposed procedure. This is due to the smaller value of the target (enforced) displacements used in pushover analysis compared to the corresponding N-LRHA displacements and due to the above reduction by the factor S_u. But at the in-plan location of CM, the floor displacements are in general marginally estimated. Slightly conservative or marginal estimates of the floor displacements from the proposed pushover procedure are observed on the stiff and flexible sides of the six-storey building. The Extended N2 pushover provides in general more conservative estimates of the floor displacements on the flexible sides of the building but also some unconservative ones on the stiff side of the first floor of the building along the II_{sec} axis.

The capacity curves of the sixteen pushovers with enforced-displacements are shown in Figure 10. The slope of the initial (elastic) branch and the ultimate and yield values of the base shear and top displacement of the building are different in each curve, depending mainly on the (±) action of the floor enforced-rotations. These curves are first bi-linearized and then can be used to connect the seismic capacity (pushover results) with the seismic demand (earthquake action) by using the informational Annex B of EN 1998-1 or any other acceptable method. By knowing the pattern of floor enforced translational displacements $\psi_{I,II}$ in elevation and the corresponding target displacement on the building top, the backwards application of EN1998-1 Annex B gives the maximum (capable) earthquake in PGA terms that the building can attain (NC state). In our case, this PGA is equal to about 0.40g, which is the same value used in N-LRHA.

Finally, the plastic mechanism of the six-storey building (which is of beam-type) is safely predicted by the envelope of the sixteen pushovers of the proposed procedure. As regards the plastic chord rotations developed at the end-sections of the structural elements, they are fully compatible with the computed interstorey drift ratios which have been in general safely estimated.
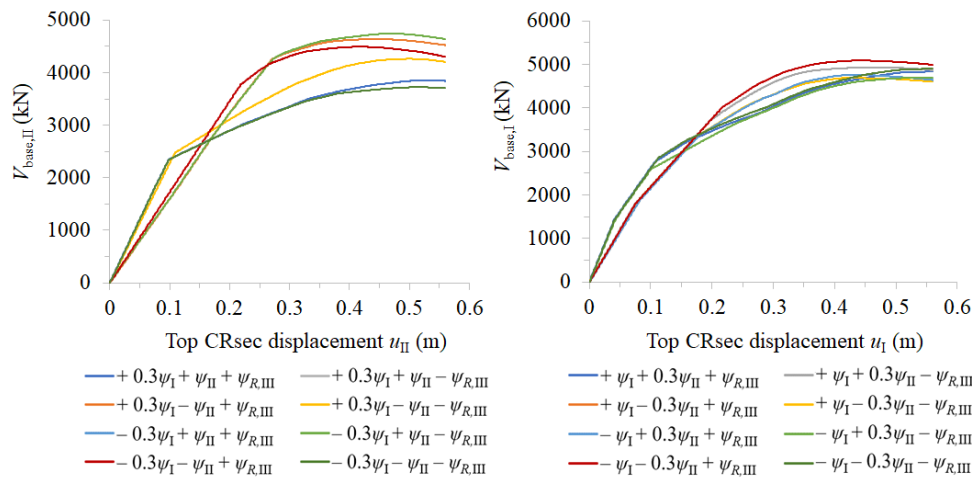

Figure 10. The 16 capacity curves of the proposed pushover procedure

4.Conclusions

An asymmetric, torsional flexible, regular in elevation, ductile, six-storey r/c building was seismically accessed here by a recently proposed pushover procedure with floor enforced-displacements to verify its effectiveness.

According to the proposed pushover procedure, a pattern of seismic floor-enforced displacements (two translational displacements and a rotational one) properly combined with each other to consider the spatial seismic action is applied and a set of sixteen pushovers is performed. The envelope of the sixteen pushovers provides a safe estimate of the seismic demand at the Near Collapse (NC) state of the building. Appropriate seismic, drift-based, floor enforced-displacements are proposed that lead the building at the attainment of the NC state. The proposed values of the floor translational displacements are further revised through two temporary sets of pushovers. All analyses

in the framework of the proposed pushover procedure are implemented with respect to an ideal, inelastic, 3D principal reference system CR_{sec} (I_{sec}, II_{sec}, III_{sec}), which is called "Capable Near Collapse Principal System of the multi-storey r/c building". This system is determined by applying the torsional optimum axis methodology to the nonlinear model of the building in which all structural members have been supplied with the secant stiffness at yield EI_{sec}. Additionally, a new criterion is used for the verification of the torsional sensitivity of the building in the non-linear area.

To verify the effectiveness of the proposed procedure on the prediction of the seismic demand, nonlinear response history analysis (N-LRHA) with 14 pairs of artificial accelerograms has been performed to provide the seismic demand at the attainment of the NC state of the six-storey r/c building. From the comparison of the response computed by the proposed pushover procedure and by the (envelope of) N-LRHA, the main conclusions are:

(a) The seismic interstorey drift-ratios on the stiff and flexible sides of the building are safely estimated by the proposed procedure. In other locations, such as those of CM and CR_{sec}, the interstorey drift ratios are marginally estimated or slightly underestimated. Hence, the main objective of the proposed procedure, which is the complete control of the distribution -in plan and in elevation- of the seismic structural damage at the NC state, is fully achieved.

(b) The seismic floor displacement profiles on the stiff and flexible sides of the building are safely estimated by the proposed procedure. In other locations, such as those of CM and CR_{sec}, the floor displacements are marginally estimated or slightly underestimated.

(c) The plastic chord rotations at the end-sections of the structural members are also safely estimated in general by the proposed procedure, following the safe estimation of the seismic interstorey drift ratios.

(d) The plastic mechanism of the building at the NC state is fully captured by the envelope of the sixteen pushover analyses in the framework of the proposed procedure.

Therefore, the proposed enforced-displacement pushover procedure is a simple and effective tool for the seismic assessment of asymmetric, torsional flexible, regular in elevation, ductile multistorey r/c buildings. The effectiveness of the proposed pushover procedure with enforced displacements has been fully evaluated in the first author's doctoral dissertation [40] by examining various regular in elevation, ductile, multistorey r/c buildings with varying number of floors, structural type, static eccentricity and torsional sensitivity. In other words, the proposed procedure can be successfully used to seismically assess any type of asymmetric multistory r/c building, torsional flexible or not, provided that are regular in elevation and develop a beam-type plastic mechanism (and not a floor-type one).

References

[1] Gupta A and Krawinkler H. (1999). Seismic demands for performance evaluation of steel moment resisting frame structures (SAC Task 5.4.3), *Report No.* 132, John A. Blume Earthq. Engineering Center, Stanford University, Stanford, CA.,
https://stacks.stanford.edu/file/druid:fm826wn5553/TR132_Gupta.pdf

[2] Goel RK (2004). Evaluation of nonlinear static procedures using building strong motion records, *In Proceedings of the 13th World Conference on Earthquake Engineering*, Paper No. 3213, 2004, 2004, August 1-6, Vancouver, B.C., Canada

[3] EN 1998-1. Eurocode 8. (2004). Design of Structures for Earthquake Resistance—Part 1: General Rules, Seismic Actions and Rules for Buildings; European Committee for Standardization: Brussels, Belgium.

[4] Bakalis A and Makarios T. (2017). Dynamic eccentricities in pushover analysis of asymmetric single-storey buildings. *In Proceedings of the Eighth European Workshop on the Seismic Behaviour of Irregular and Compex Structures*, Bucharest, Romania, 19–20 October 2017.

[5] Bakalis A and Makarios T. (2018). Dynamic eccentricities and the "capable near collapse centre of stiffness" of reinforced concrete single-storey buildings in pushover analysis. *Engineering Structures*, 166: 62–78.
https://doi.org/10.1016/j.engstruct.2018.03.056

[6] Bakalis A and Makarios T. (2019). Seismic

assessment of asymmetric single-story RC buildings by modified pushover analysis using the "Capable Near Collapse Centre of Stiffness": Validation of the method. Journal of Earthquake Engineering. https://doi.org/10.1080/13632469.2019.1698477

[7] Bakalis AP and Makarios TK. (2020). Dynamic eccentricities in pushover analysis of asymmetric single-storey buildings, In: Köber D., De Stefano M., Zembaty Z. (eds) Seismic Behaviour and Design of Irregular and Complex Civil Structures III. Geotechnical, Geological and Earthquake Engineering, vol 48. Springer, Cham. https://doi.org/10.1007/978-3-030-33532-8_24

[8] Bakalis A and Makarios T. (2021). Seismic Enforced-Displacement pushover procedure on multistorey R/C buildings. *Engineering Structures*, 229. https://doi.org/10.1016/j.engstruct.2020.111631

[9] Makarios T and Bakalis A. (2018). Pushover analysis using suitable dynamic eccentricities on asymmetric single-storey buildings. *In Proceedings of the 16th European Conference of Earthquake Engineering*, Thessaloniki, Greece, 18–21 June 2018. http://www.16ecee.org/proceedings

[10] Makarios T and Bakalis A. (2020). Seismic enforced displacement-based pushover analysis on irregular in-plan R/C multistorey buildings, *In Proceedings of Ninth European Workshop on the Seismic Behaviour of Irregular and Complex Structures*, p. 12, December 15-16, Lisbon, Portugal. https://ceris.pt/event/9th-european-workshop-on-the-seismic-behaviour-of-irregular-and-complex-structures/

[11] Makarios TK and Bakalis AP. (2022). Seismic Enforced Displacement-Based Pushover Analysis on Irregular In-Plan R/C Multi-storey Buildings. In: Bento, R., De Stefano, M., Köber, D., Zembaty, Z. (eds) *Seismic Behaviour and Design of Irregular and Complex Civil Structures IV. Geotechnical, Geological and Earthquake Engineering*, vol 50. Springer, Cham. https://doi.org/10.1007/978-3-030-83221-6_3

[12] Bakalis A, Makarios T and Athanatopoulou A. (2021). Inelastic dynamic eccentricities in pushover analysis procedure of multi-story RC buildings. *Buildings*, 11(5), 195.

https://doi.org/10.3390/buildings11050195

[13] Chopra AK and Goel RK. (2004). A modal pushover analysis procedure to estimate seismic demands for unsymmetric-plan buildings. *Earthquake Engng Struct Dyn*; 33(8):903–27, https://doi.org/10.1002/eqe.380

[14] Reyes JC and Chopra AK. (2011). Three-dimensional modal pushover analysis of buildings subjected to two components of ground motion, including its evaluation for tall buildings. *Earthquake Engin. Struct. Dyn*., 40: 789–806, https://doi.org/10.1002/eqe.1060

[15] Hernandez-Montes E, Kwon OS and Aschheim MA. (2004). An energy-based formulation for first and multiple-mode nonlinear static (pushover) analyses. *J Earthquake Eng*, 8(01): 69–88, https://doi.org/10.1080/13632460409350481

[16] Lin JL and Tsai KC. (2008). Seismic analysis of two-way asymmetric building systems under bi-directional seismic ground motions. *Earthquake Engng. Struct*. Dyn., 37: 305-328, https://doi.org/10.1002/eqe.759

[17] Manoukas G, Athanatopoulou A and Avramidis I. (2012). Multimode pushover analysis for asymmetric buildings under biaxial seismic excitation based on a new concept of the equivalent single degree of freedom system. *Soil Dynamics and Earthquake Engineering*, 38: 88-96. https://doi.org/10.1016/j.soildyn.2012.01.018

[18] Fujii K. (2014). Prediction of the largest peak nonlinear seismic response of asymmetric buildings under bi-directional excitation using pushover analyses. *Bull Earthquake Eng*, 12: 909–938, https://doi.org/10.1007/s10518-013-9557-x

[19] Soleimani S, Aziminejad A and Moghadam AS. (2017). Extending the concept of energy-based pushover analysis to assess seismic demands of asymmetric-plan buildings. *Soil Dynamics and Earthquake Engineering*, 93: 29–41. http://dx.doi.org/10.1016/j.soildyn.2016.11.014

[20] Fajfar P, Marusic D and Perus I (2005). Torsional effects in the pushover-based seismic analysis of buildings. *Journal of Earthquake Engineering*, 9 (6): 831–54, https://doi.org/10.1080/13632460509350568

[21] Kreslin M and Fajfar P (2012). The extended N2

method considering higher mode effects in both plan and elevation. *Bull Earthquake Eng*, 10: 695-715. https://doi.org/10.1007/s10518-011-9319-6

[22] Bhatt C and Bento R (2011). Extension of the CSM-FEMA440 to plan-asymmetric real building structures. *Earthquake Eng Struct Dyn*, 40(11): 1263–82, https://doi.org/10.1002/eqe.1087

[23] Rofooei FR and Mirjalili MR (2018). Dynamic-based pushover analysis for one-way plan-asymmetric buildings. *Engineering Structures*, 163:332-346. https://doi.org/10.1016/j.engstruct.2018.02.052

[24] Bosco M, Ghersi A and Marino EM (2012). Corrective eccentricities for assessment by the nonlinear static method of 3D structures subjected to bidirectional ground motions. *Earthq Eng Struct Dyn*, 41:1751–73. http://dx.doi.org/10.1002/eqe.2155

[25] Bosco M, Ghersi A, Marino EM and Rossi PP (2017). Generalized corrective eccentricities for nonlinear static analysis of buildings with framed or braced structure. *Bull Earthq Eng*, 15: 4887–4913. http://dx.doi.org/10.1007/s10518-017-0159-x

[26] Antoniou S and Pinho R (2004a). Advantages and limitations of adaptive and non-adaptive force-based pushover procedures. *Journal of Earthquake Engineering*, 8(4): 497–522, https://doi.org/10.1142/S1363246904001511

[27] Antoniou S and Pinho R. (2004b). Development and verification of a displacement-based adaptive pushover procedure. *Journal of Earthquake Engineering*, 8(5): 643–661, https://doi.org/10.1080/13632460409350504

[28] Kalkan E and Kunnath SK. (2006). Adaptive modal combination procedure for nonlinear static analysis of building structures. ASCE, *J Struct Eng*, 132(11): 1721–1731, https://doi.org/10.1061/(ASCE)0733-9445(2006)132:11(1721)

[29] Bhatt C and Bento R. (2014). The Extended Adaptive Capacity Spectrum Method for the seismic assessment of plan-asymmetric buildings. *Earthquake Spectra*, 30(2): 683-703, https://doi.org/10.1193%2F022112EQS048M

[30] Amini MA and Poursha M. (2018). Adaptive force-based multimode pushover analysis for seismic evaluation of midrise buildings. *Journal of Structural Engineering*, Vol. 144, Issue 8. https://doi.org/10.1061/(ASCE)ST.1943-541X.0002070

[31] Poursha M, Khoshnoudian F and Moghadam AS. (2014). The extended consecutive modal pushover procedure for estimating the seismic demands of two-way unsymmetric-plan tall buildings under influence of two horizontal components of ground motions. *Soil Dynamics and Earthquake Engineering*, 63: 162-173. https://doi.org/10.1016/j.soildyn.2014.02.001

[32] Goel RK (2004). Evaluation of nonlinear static procedures using building strong motion records, *In Proceedings of the 13th World Conference on Earthquake Engineering*, Paper No. 3213, 2004, 2004, August 1-6, Vancouver, B.C., Canada

[33] Goel RK and Chopra AK. (2004). Evaluation of modal and FEMA pushover analyses: SAC buildings. *Earthquake spectra*, 20(1): 225–54. https://doi.org/10.1193%2F1.1646390

[34] Erduran E. (2008). Assessment of current nonlinear static procedures on the estimation of torsional effects in low-rise frame buildings. *Eng. Struct.*, 30(9): 2548-2558. https://doi.org/10.1016/j.engstruct.2008.02.008

[35] Baros DK and Anagnostopoulos SA (2008). An overview of pushover procedures for the analysis of buildings susceptible to torsional behavior, *In proceedings of the 14th World Conference on Earthquake Engineering*, 2008, October 12-17, Beijing, China, http://www.iitk.ac.in/nicee/wcee/article/14_05-01-0195.PDF

[36] Bento R, Bhatt C and Pinho R. (2010). Using nonlinear static procedures for seismic assessment of the 3D irregular SPEAR building. *Earthq. Struct.*, 1(2): 177-195, https://doi.org/10.12989/eas.2010.1.2.177

[37] Bhatt C and Bento R (2012). Comparison of nonlinear static methods for the seismic assessment of plan irregular frame buildings with non seismic details. *J. Earthq. Eng.*, 16(1): 15-39, https://doi.org/10.1080/13632469.2011.586085

[38] De Stefano M and Mariani V. (2014). Pushover analysis for plan irregular building structures, In: Ansal A. (eds) *Perspectives on European Earthquake Engineering and Seismology. Geotechnical, Geological and Earthquake Engineering*, vol 34. Springer, Cham. https://doi.org/10.1007/978-3-319-07118-3_13

[39] Anagnostopoulos SA, Kyrkos MT and Stathopoulos KG. (2015). Earthquake induced torsion in buildings: critical review and state of the art. *Earthquakes and Structures*, 8(2): 305–377. https://doi.org/10.12989/EAS.2015.8.2.305

[40] Bakalis A. (2021). "*Seismic non-linear static analysis of asymmetric reinforced concrete buildings at capable near collapse state using imposed floor displacements or inelastic dynamic eccentricities*". PhD dissertation (in greek). School of Civil Engineering of Aristotle University of Thessaloniki. Greece, https://freader.ekt.gr/eadd/index.php?doc = 49775 &lang = el

[41] EN 1998-3. Eurocode 8, (2005). Design of Structures for Earthquake Resistance—Part 3: Assessment and Retrofitting of Buildings; European Committee for Standardization: Brussels, Belgium.

[42] Makarios T and Anastassiadis K. (1998a). Real and fictitious elastic axis of multi-storey buildings: theory. *Struct Des Tall Build* 1998;7(1):33–55, https://doi.org/10.1002/(SICI)1099-1794 (199803)7:1%3C33::AID-TAL95%3E3.0.CO;2-D

[43] Makarios T and Anastassiadis K. (1998b). Real and fictitious elastic axis of multi-storey buildings: applications. *Struct Des Tall Build*;(1):57–71, https://doi.org/10.1002/(SICI)1099-1794 (199803)7:1%3C57::AID-TAL96%3E3.0.CO;2-0

[44] Makarios T. (2005). Optimum torsion axis to multistory buildings by using the continuous model of the structure. *J Struct Des Tall Spec Build*;14(1):69–90, https://doi.org/10.1002/tal.262

[45] Makarios T. (2008). Practical calculation of the torsional stiffness radius of multistorey tall buildings. *J Struct Des Tall Spec Build* 2008;17(1):39–65, https://doi.org/10.1002/tal.316

[46] Makarios T, Athanatopoulou AM and Xenidis H. (2006). Numerical verification of properties of the fictitious elastic axis in asymmetric multistorey buildings. *J Struc Des Tall Spec Build*;15(3):249–76, https://doi.org/10.1002/tal.294

[47] Athanatopoulou A and Doudoumis I. (2008). Principal directions under lateral loading in multistory asymmetric buildings. *Struct Des Tall Spec Build*;17(4):773–94, http://dx.doi.org/10.1002/tal.385

[48] Marino E and Rossi P. (2008). Exact evaluation of the location of the optimum torsion axis. *Struct Des Tall Spec Build* 2004;14(4):277–90, https://doi.org/10.1002/tal.252

[49] Georgoussis G. (2006). Modal eccentricities of asymmetric structures. *Struct Des Tall Spec Build*;15:339–361, https://doi.org/10.1002/tal.299

[50] Georgoussis G. (2009). An alternative approach for assessing eccentricities in asymmetric multistory buildings.1. Elastic systems. *Struct Des Tall Spec Build*: vol.18, issue 2, 181-202, https://doi.org/10.1002/tal.401

[51] Georgoussis G. (2010). Modal rigidity center: it's use for assessing elastic torsion in asymmetric buildings. Techno-press: *Earthquakes Struct J*; vol.1, issue 2:163–175, https://doi.org/10.12989/eas.2010.1.2.163

[52] Bosco M, Marino EM and Rossi PP. (2013). An analytical method for the evaluation of the in plan irregularity of non-regularity asymmetric buildings. *Bull Earthq Eng* 2013;11(5):1423–45, http://dx.doi.org/10.1007/s10518-013-9438-3

[53] Hejal R and Chopra, AK. (1987). Earthquake Response of Torsionally-Coupled Buildings; *Report No. UCB/EERC-87-20; Earthquake Engineering Research Center*, University of California: Berkeley, CA, USA, 1987, https://nisee.berkeley.edu/elibrary/eerc/1987

[54] EN 1992-1-1. Eurocode 2. (2004). Design of concrete structures - Part 1-1: General rules and rules for buildings [Authority: The European Union Per Regulation 305/2011, Directive 98/34/ EC, Directive 2004/18/EC].

[55] SAP2000-CSI. (2022). Three dimensional static and dynamic finite element analysis and design

of structures V23. *Computers and Structures Inc.* Berkeley, CA, USA.

[56] Mander JB, Priestley MJN and Park R. (1988). Theoretical stress-strain model for confined concrete. *J Struct Eng*; 114(8):1827–49. https://doi.org/10.1061/(ASCE)0733-9445(1988) 114:8(1804)

[57] Park R and Paulay T. (1975). *Reinforced concrete structures*. New York: John Wiley & Sons, Inc.; https://onlinelibrary.wiley.com/doi/book/10.1002/ 9780470172834

[58] Seismosoft-SeismoArtif. (2016). A Computer Program for Generating Artificial Earthquake Accelerograms Matched to a Specific Target

Response Spectrum; Seismosoft SRL: Pavia, Italy. https://seismosoft.com/products/seismoartif/

[59] Makarios T. (2015). Design Characteristic value of the Arias intensity magnitude for artificial accelerograms compatible with Hellenic seismic hazard zones. *Int. J. Innov. Res. Adv. Eng.*, 2, 87–98, http://www.ijirae.com/volumes/Vol2/iss1/14.JACE 10085.pdf

[60] Fajfar P (2000). A nonlinear analysis method for performance-based seismic design. *Earthquake Spectra*, 16(3): 573-592, https://doi.org/10.1193%2F1.1586128

Appendix A

Figure A1 shows the numbering of the structural members in the nonlinear model of the six-storey r/c building. The dimensions of the cross-sections and the reinforcement details are presented in Tables A1-A3.
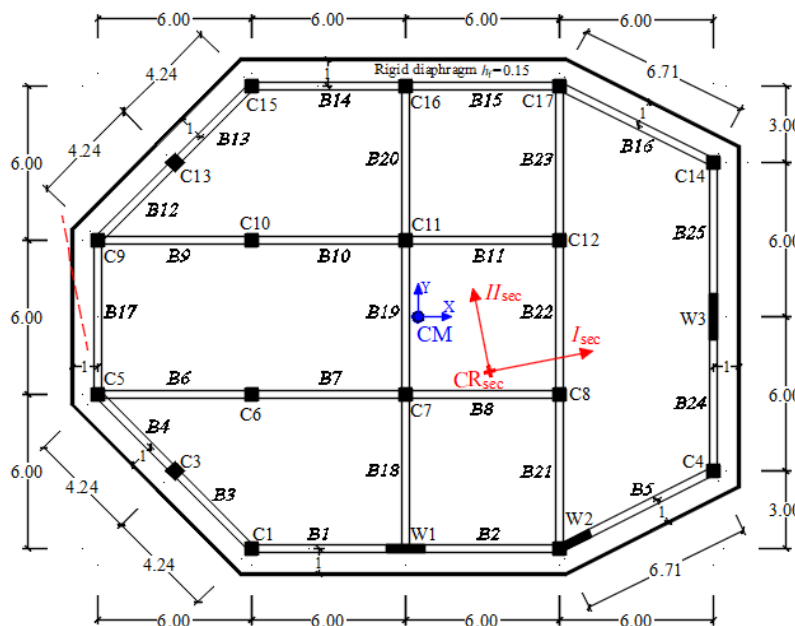
Figure A1. Numbering of the structural members in the nonlinear model of the six-storey r/c building

Table A1. Geometry of cross sections

Structural element	Storey					
	1	2	3	4	5	6
All square columns	50/50					
All **T**-beams	**T** 30/60/150/15					
Wall W1	150/30					
Wall W2	150/30/50/50					
Wall W3	30/180					

Table A2. Reinforcement details of **T** beams' end-sections (closed perimeter stirrup Ø8mm placed every 80mm).

Top flange reinforcement bars: 12Ø8mm (Ø8/120mm) are considered in the calculation of the bending strength of T beams.

Beam	Storey											
	1		2		3		4		5		6	
	start	end	start	end	start	end	start	end	start	end	start	end
	Longitudinal bars Ø16mm or Ø14mm (*) at beam end-sections, placed on top-bottom fibers											
B 1	6-5	8-6	7-5	9-7	7-5	9-7	5-4	7-5	5-4 *	5-4	4-4 *	4-4 *
2	8-6	9-7	9-7	10-8	9-7	9-7	7-5	8-6	5-4	6-5	4-4 *	4-4
3	4-4	4-4	5-5	5-5	5-5	5-5	4-4	4-4	4-4 *	4-4 *	4-4 *	4-4 *
4	4-4	4-4	5-5	5-5	5-5	5-5	4-4	4-4	4-4 *	4-4 *	4-4 *	4-4 *
5	6-5	6-5	8-6	7-6	8-6	7-6	6-5	5-5	4-4	4-4	4-4 *	4-4 *
6	5-4	5-4	5-4	6-5	5-4	6-5	4-4	4-4	4-4 *	4-4	4-4 *	4-4 *
7	5-4	5-4	6-5	6-5	6-5	6-5	4-4	4-4	4-4	4-4 *	4-4 *	4-4 *
8	5-4	5-4	6-5	6-5	6-5	6-5	4-4	4-4	4-4 *	4-4 *	4-4 *	4-4 *
9	5-4	6-4	6-4	6-4	5-4	6-4	4-4	5-4	4-4 *	4-4	4-4 *	4-4 *
10	6-4	6-4	6-4	6-4	6-4	5-4	5-4	4-4	4-4	4-4 *	4-4 *	4-4 *
11	6-4	6-5	6-4	7-5	5-4	6-5	4-4	5-4	4-4 *	4-4 *	4-4 *	4-4 *
12	5-5	5-4	5-5	6-4	4-4	5-4	4-4	4-4	4-4 *	4-4 *	4-4 *	4-4 *
13	5-4	6-5	6-4	6-5	5-4	5-4	4-4	4-4	4-4 *	4-4 *	4-4 *	4-4 *
14	7-5	6-5	7-5	7-5	7-5	6-5	5-4	5-4	4-4	4-4 *	4-4 *	4-4 *
15	6-5	6-5	7-5	7-5	6-5	6-5	5-4	5-4	4-4 *	4-4 *	4-4 *	4-4 *
16	7-5	8-6	8-6	8-6	7-5	7-5	6-5	6-5	4-4	4-4	4-4 *	4-4 *
17	4-4	4-4	5-4	5-4	5-4	5-4	5-4	5-4	4-4	4-4	4-4 *	4-4 *
18	4-4	4-4	4-4	4-4	4-4	4-4	4-4	4-4	4-4	4-4	4-4 *	4-4 *
19	4-4	4-4	4-4	4-4	4-4	4-4	4-4	4-4	4-4	4-4	4-4 *	4-4 *
20	4-4	4-4	4-4	4-4	4-4	4-4	4-4	4-4	4-4	4-4	4-4 *	4-4 *
21	4-4	4-4	5-4	5-4	5-4	4-4	4-4	4-4	4-4	4-4	4-4 *	4-4 *
22	4-4	4-4	5-4	5-4	4-4	4-4	4-4	4-4	4-4	4-4	4-4 *	4-4 *
23	4-4	4-4	5-4	4-4	4-4	4-4	4-4	4-4	4-4	4-4	4-4 *	4-4 *
24	7-6	8-6	8-6	9-7	8-6	9-7	7-6	8-6	5-4	5-4	4-4 *	4-4
25	8-6	7-5	9-7	8-6	9-7	8-6	8-6	7-6	5-4	5-4	4-4	4-4 *

Table A3. Reinforcement details of columns and walls

Column (C) or Wall (W)	Storey					
	1	2	3	4	5	6
	Number of longitudinal bars and diameter (mm). *Number of (closed) stirrup legs along x and y dir. - diameter (mm) / distance (mm) between legs*					
All columns	12Ø20 confinement x & y: 4 legs - Ø8/80					4Ø20+8Ø14 x & y: 4 legs - Ø8/80
W1	2 b. el. 0.4x0.3m: (3Ø25+7Ø20) x 2 web: 10Ø10 confinement x, y: 4, 6 legs - Ø8/80	2 boundary el. 0.4x0.3m: (10Ø14) x 2 web: 10Ø10 confinement x, y: 4, 6 legs - Ø8/80				
W2	2 boundary el. 0.5x0.5m + 0.4x0.3m: (16Ø20) + (3Ø25+7Ø20) web: 10Ø10 confinement x, y: (6, 6 legs - Ø8/80) + (6, 6 legs - Ø8/80)					2 b. el. 0.5x0.5m + 0.4x0.3m: (12Ø20) + (10Ø14) web: 10Ø10 confinement x, y: (4, 4 legs - Ø8/80) + (4, 6 legs - Ø8/80)
W3	2 b. el. 0.3x0.45m: (12Ø20) x 2 web: 14Ø12 confinement x, y: 6, 4 legs - Ø8/80	2 b. el. 0.3x0.40m: (10Ø20) x 2 web: 12Ø12 confinement x, y: 6, 4 legs - Ø8/80				2 bound. el. 0.3x0.40m: (10Ø14) x 2 web: 12Ø12 confinement x, y: 6, 4 legs - Ø8/80